On Adaptive Definition of the Plane Wave Basis for Wave Boundary Elements in Acoustic Scattering: the 2D Case

J. Trevelyan[1] and G. Coates[1]

Abstract: The terminology "wave boundary elements" relates to boundary elements enriched in the Partition of Unity sense by a multiple plane wave basis for the analysis of the propagation of short wavelength waves. This paper presents a variant of this approach in which the plane wave basis is selected adaptively according to an error indicator. The error indicator is residual based, and exhibits useful local and global properties. Model improvement in each adaptive iteration is carried out by the addition of new plane waves with no *h*-refinement. The convergence properties of the scheme are demonstrated.

Keywords: wave scattering, plane wave basis, boundary integral equation, boundary elements, adaptivity.

1 Introduction

This paper deals with the efficient solution of frequency domain boundary value problems in wave propagation. Finite element and boundary element schemes have, of course, become well established as tools to carry out such simulations. However, users of conventional schemes, i.e. those schemes using a polynomial shape function basis, are well known to be constrained by a heuristic rule that prescribes a maximum nodal spacing of approximately $\lambda/10$, where λ is the wavelength under consideration. Similar restrictions are found in meshless methods, e.g. Soares (2009). This places a de facto upper bound on the frequency that may be considered for any given problem given a finite computational resource. For many problems of practical scientific and engineering interest, e.g. radar scattering by an aircraft, this limitation presents an obstacle to the effective usage of element-based methods.

Attempts to increase the upper bound on frequency have been the subject of active research over the last decade. Fast multipole methods (FMM) (Chew, Jin, Michielssen, and Song (1997); Darve (2000), for example) present a promising avenue of research. For a problem containing N nodes, the N^2 nodal interactions

---

[1] School of Engineering & Computing Sciences, Durham University, UK.

through the Green's function are expanded in a multipole expansion so that the total number of computations is greatly reduced, and giving rise to acceleration in the matrix vector products that are central to the iterative solution of large systems. Adaptive Cross Approximation (ACA) (Bebendorf (2000)) is an alternative technique for accelerating boundary element matrices for general applications; this has been applied to wave problems by Brancati, Aliabadi, and Benedetti (2009). The matrix is partitioned hierarchically in such a way that each partition may be accurately expressed as a low rank approximation implemented as a convergent series of vector operations.

Without prejudice against FMM and ACA, both of which are likely to be orthogonal to the methods presented herein, the current paper focuses on a class of methods in which the wave potential is sought in some wave basis. Abboud, Nédélec, and Zhou (1995) showed that, for convex scatterers impinged by an incident wave of sufficiently high frequency, the scattered potential may be efficiently approximated as the product of a slowly varying function and the incident wave itself. The slowly varying function may then be approximated using a piecewise polynomial finite element or boundary element space. This has been shown to provide "wavenumber independent" complexity, e.g. Bruno, Geuzaine, Munro, and Reitich (2004) present results for scatterers of dimension $10^6 \lambda$. Langdon and Chandler-Wilde (2006) show that the approach is suitable for polygonal scatterers. Anand, Boubendir, Ecevit, and Reitich (2006) extended the approach to scattering by two or more objects. Dominguez, Graham, and Smyshlyaev (2007) showed that, for asymptotically high wave numbers, the number of degrees of freedom needs to grow only with $\mathcal{O}(k^{1/9})$ to maintain a fixed error bound (the reader is reminded that wave number $k = 2\pi/\lambda$). It should be recalled that these methods are limited to convex scatterers and may not perform well if λ is not very small in comparison with the scatterer, i.e. for low or medium frequency problems.

The extension of these ideas to consider a basis comprising multiple plane waves was proposed, without confirming examples, by de la Bourdonnaye (1994) for integral equation methods in wave simulation. The Partition of Unity Method (PUM) of Melenk and Babuška (1996) generalised the use of approximation spaces comprising sets of functions known to populate the solution space for any differential equation under consideration. Sets of plane waves were proposed for wave problems. When applied to finite element and boundary element approximations for waves, the PUM results in a reformulation of the problem so that we no longer seek the solution in terms of the nodal values of potential, but instead solve for the amplitudes of a set of approximating plane waves at each node that may be linearly combined to recover the potential field. Papers describing the Partition of Unity Finite Element Method (PU-FEM) for wave problems have appeared in the

literature, including Laghrouche, Bettess, and Astley (2002); Laghrouche, Bettess, Perrey-Debain, and Trevelyan (2003); Ortiz and Sanchez (2000), and the approach is also seen in the discontinuous enrichment method (see, for example, Farhat, Harari, and Franca (2001); Massimi, Tezaur, and Farhat (2008)), the generalized finite element method of Strouboulis, Babuška, and Hidajat (2006), the ultraweak variational formulation of Cessenat and Després (1998) and the Variational Theory of Complex Rays (VTCR) of Riou, Ladevèze, and Sourcis (2008). Following the initial proposition by de la Bourdonnaye (1994) of a multiple plane wave basis in a boundary integral equation, the approach was further developed in a series of papers by Perrey-Debain, Trevelyan, and Bettess (2002, 2003a,b) and Perrey-Debain, Laghrouche, Bettess, and Trevelyan (2004), considering Helmholtz problems and elastic waves. These authors showed that the plane wave expansion reduced the required number of degrees of freedom to approximately 2.5 per wavelength, a marked reduction over the 10 per wavelength required with the polynomial basis while retaining 'engineering accuracy', as defined by 1% $L^2(\Gamma)$ norm of the relative error in comparison with an analytical solution. The inclusion of the PUM in a boundary element context may be termed PU-BEM, and the elements that are enriched in this way may be termed wave boundary elements.

Although recent advances have been made in the numerical integration of oscillatory functions (Huybrechs and Vandewalle (2006); Trevelyan (2007); Honnor, Trevelyan, and Huybrechs (2009); Trevelyan and Honnor (2009); Kim, Dominguez, Graham, and Smyshlyaev (2009)), the run time in the PU-BEM is dominated by the evaluation of boundary integrals. It becomes important, therefore, to optimise carefully the number of plane waves used in the basis at each node to minimise the total number of boundary integrals required to be considered. For general problems, in which an analytical solution is not available and the optimal local enrichment varies over the scatterer boundary, an adaptive scheme appears attractive for definition of the basis. Some initial experiments were reported at conferences by Trevelyan, Bettess, and Perrey-Debain (2004) for the PU-BEM and by Ladevèze, Sourcis, Riou, and Faverjon (2008) for the Variational Theory of Complex Rays (VTCR). Chandrasekhar and Rao (2008) have presented adaptive edge basis functions for a Method of Moments solution for acoustic scattering. This paper presents a fuller exposition of adaptivity in PU-BEM with appropriate error indicators.

Section 2 of this paper presents the PU-BEM for Helmholtz problems, and Section 3 presents the adaptive scheme that is the main novel component of the work. Section 4 contains some more detailed notes on implementation of the algorithms. Section 5 describes some results for two test cases, and some concluding remarks are made in Section 6.

2   Partition of Unity Boundary Element Method for wave propagation

We consider a domain $\Omega \in \mathbb{R}^2$, unbounded in the exterior and bounded internally by a scatterer of boundary $\partial\Omega = \Gamma$. Assuming $e^{-i\omega t}$ time dependence, the wave equation reduces to the familiar Helmholtz equation form

$$(\nabla^2 + k^2)\phi(x) = 0, \quad x \in \Omega \tag{1}$$

where ∇^2 is the Laplacian operator, k is the wavenumber, given by $2\pi/\lambda$, and we seek the complex potential field $\phi(x)$. This paper is aimed specifically at problems characterised by medium to large k, such that the frequency is sufficiently high that conventional FEM and BEM formulations become impractical, but not so high that asymptotic methods apply. Let the scatterer be impinged by an incident wave $\phi^I(x) = A^I e^{ik\psi^I \cdot x}$, i.e. a plane wave of amplitude $A^I \in \mathbb{C}$ travelling in the direction described by unit vector ψ^I. Transformation of the governing differential equation into an equivalent boundary integral equation (BIE) form is standard (e.g. Brebbia and Ciskowski (1991)), arriving at

$$c(x_0)\phi(x_0) + \int_\Gamma \frac{\partial G(x,x_0)}{\partial n}\phi(x)d\Gamma(x) = \int_\Gamma G(x,x_0)\frac{\partial \phi(x)}{\partial n}d\Gamma(x) + \phi^I(x_0), \quad x_0 \in \Gamma \tag{2}$$

where c is a scalar dependent on the boundary geometry at point x_0, n is the unit outward-pointing normal at boundary point x, and G is the Green's function, which for the Helmholtz equation is given by

$$G(x,x_0) = \frac{i}{4}H_0(kr). \tag{3}$$

Here $r := |x - x_0|$ is the usual radial coordinate in boundary element methods, and $H_0(\cdot)$ is a Hankel function of the first kind and of order 0. Considering a general form of boundary condition to be applied, given by

$$\frac{\partial \phi(x)}{\partial n} = \alpha(x)\phi(x) + \beta(x), \quad x \in \Gamma \tag{4}$$

the BIE may be reformulated as

$$c(x_0)\phi(x_0) + \int_\Gamma \left(\frac{\partial G(x,x_0)}{\partial n} - G(x,x_0)\alpha(x) \right)\phi(x)d\Gamma(x)$$
$$= \int_\Gamma G(x,x_0)\beta(x)d\Gamma(x) + \phi^I(x_0) \tag{5}$$

Here, for compact presentation we take the case of a perfectly reflecting ("sound-hard") scatterer, so $\alpha(x) = \beta(x) = 0, x \in \Gamma$, leading to a BIE in only the double layer potential,

$$c(x_0)\phi(x_0) + \int_\Gamma \frac{\partial G(x,x_0)}{\partial n}\phi(x)d\Gamma(x) = \phi^I(x_0). \tag{6}$$

However, the approach extends in an identical fashion to sound-soft or impedance boundary conditions. In the direct collocation BEM, the boundary Γ is discretised and each element of boundary Γ_e considered in an intrinsic coordinate system through the usual parameterisation of a finite/boundary element, i.e.

$$\Gamma_e = \{\gamma_e(\xi) : \xi \in [-1,1]\} \tag{7}$$

where $\gamma_e : \mathbb{R} \to \mathbb{R}^2$. For any element, the mapping between $x \in \Gamma$ and ξ is unique and bidirectional, and it shall be henceforth assumed that any function $f(x)$ is equivalent to $f(\xi)$ as suggested by this mapping. Expressing the potential in a piecewise polynomial basis over element e,

$$\phi(x) = \sum_{j=1}^{J} N_j(x)\phi_j^e \tag{8}$$

where J is the number of nodes per element, N_j is the Lagrangian shape function for node j and ϕ_j^e is the unknown nodal potential at node j on element e, we write

$$c(x_0)\phi(x_0) + \sum_{e=1}^{E}\sum_{j=1}^{J}\int_{-1}^{+1}\frac{\partial G(x,x_0)}{\partial n}N_j(\xi)J^n(\xi)d\xi\,\phi_j^e = \phi^I(x_0) \tag{9}$$

where E is the total number of elements, and J^n is the Jacobian of the mapping (7). Collocating this discretised statement of the BIE at a sufficient number of points $x_0 \in \Gamma$ yields a system of linear equations that may be solved for the nodal potentials in the conventional fashion. Some method needs to be employed to overcome the problem posed by the non-uniqueness of the solution to (6) at the eigenfrequencies of the associated interior Dirichlet problem (Schenck (1968); Burton and Miller (1971)); the current authors use the method of Schenck (1968) for reasons of computational efficiency but modified in a similar fashion to Mohsen and Hesham (2006) to retain a square system. To move from the classical direct collocation BEM to the PU-BEM, we introduce the plane wave expansion of the potential on an element e,

$$\phi(x) = \sum_{j=1}^{J} N_j(x)\sum_{m=1}^{M} A_{jm}^e e^{ik\psi_{jm}^e \cdot x}, \quad |\psi_{jm}^e| = 1 \tag{10}$$

where $A^e_{jm} \in \mathbb{C}$ and $\psi_{jm} \in \mathbb{R}^2$ are, respectively, the amplitudes and directions of the plane waves in the basis. For nodes that are shared between adjacent elements, the same plane wave basis is considered for each element, and the amplitudes of the individual waves are taken to be identical, providing for C^0 continuity in potential across element interfaces. M may be chosen such that, for any given mesh, requirements on the number of degrees of freedom per wavelength, τ, are observed both globally and locally. We recall that $\tau \geq 10$ is generally observed for FEM and BEM approximations; Perrey-Debain, Trevelyan, and Bettess (2003a) have shown that a considerably coarser discretisation of $\tau \simeq 2.5$ is sufficient for PU-BEM. In general, τ may be allowed to reduce further towards 2.0 as the frequency increases. Substitution of (10), instead of (8), into (6) results in the BIE being reformulated such that the unknowns become the amplitudes A^e_{jm}.

$$c(x_0)\phi(x_0) + \sum_{e=1}^{E} \sum_{j=1}^{J} \sum_{m=1}^{M} \int_{-1}^{+1} \frac{\partial G(x,x_0)}{\partial n} N_j(\xi) e^{ik\psi^e_{jm}\cdot x} J^n(\xi) d\xi A^e_{jm} = \phi^I(x_0) \qquad (11)$$

There become M degrees of freedom associated with each node, and so collocation only at the nodes will provide an insufficient number of equations; an auxiliary set of equations is provided by collocating at a sufficient number of non-nodal points distributed over the boundary. To accomplish this, the potential at the collocation point, $\phi(x_0)$, in (11) needs to be written in the expansion (10),

$$\phi(x_0) = \sum_{j=1}^{J} N_j(x_0) \sum_{m=1}^{M} A^{\bar{e}}_{jm} e^{ik\psi^{\bar{e}}_{jm}\cdot x_0} \qquad (12)$$

where $\bar{e}$ is the element on which x_0 lies. This yields a square system of linear equations

$$[W + K]\{a\} = \{b\} \qquad (13)$$

where the sparse square matrix W results from interpolation of the plane waves through (12) and square matrix K is fully populated with the boundary integrals contained in (11). Right hand side vector b contains the incident wave potentials at the collocation points, and the unknown vector a contains the amplitudes A^e_{jm}. The amplitudes may be determined through solution of the system (13), being careful to use a solver appropriate to the conditioning of $[W + K]$, and the potential field may quickly be recovered through (10). If required, solutions in the domain Ω (e.g. for the far-field pattern) may be found by making further use of (11) in the usual way. In most PU-BEM works in the literature, and cited in this article, the wave directions ψ^e_{jm} have been simply defined to be equally spaced around the unit circle,

i.e.

$$\psi_{jm}^e = (cos\theta_{jm}^e, sin\theta_{jm}^e), \qquad \theta_{jm}^e = \frac{2\pi(m-1)}{M} + \delta\theta \qquad (14)$$

In order to represent the physical optics solution for large k, we take the offset $\delta\theta$ to be the direction of the incident wave. We note that, while the number of waves, M, is generally much more important than the direction vectors ψ_{jm}^e, the results do exhibit some sensitivity to the basis directions chosen. Selection of a wave basis that is in some sense optimal for the problem in question is an open research question (see Bériot, Perrey-Debain, Ben Tahar, and Vayssade (2010)). In the following section we show how this set of wave directions is augmented iteratively to enhance the solution.

3   Adaptive scheme

The core elements of most adaptive schemes found in the FE and BE literature are an error indicator and some strategy, generally h or p, for model improvement. The current work is no exception. This section presents such a scheme, of the p-adaptive character, for 2D PU-BEM approximations. In this scheme, the number of plane waves in the basis at node j of element e, now denoted M_{ej}, varies with j. Thus the BIE (11) may be presented in the slightly modified form,

$$c(x_0)\phi(x_0) + \sum_{e=1}^{E}\sum_{j=1}^{J}\sum_{m=1}^{M_{ej}}\int_{-1}^{+1}\frac{\partial G(x,x_0)}{\partial n}N_j(\xi)e^{ik\psi_{jm}^e\cdot x}J^n(\xi)d\xi A_{jm}^e = \phi^I(x_0) \qquad (15)$$

In successive iterations of the adaptive scheme, the approximation space is progressively enriched by the addition of plane waves by incrementing the value M_{ej} at any node(s) selected by a local error indicator.

A residual based error indicator R may be defined as,

$$R(x_1) := \frac{1}{|A^I|}\left|c(x_1)\phi(x_1) + \int_{\Gamma}\frac{\partial G(x,x_1)}{\partial n}\phi(x)d\Gamma(x) - \phi^I(x_1)\right|, \qquad x_1 \in \Gamma \qquad (16)$$

where the integral term may be evaluated in the same discrete form as in (15)

$$\int_{\Gamma}\frac{\partial G(x,x_1)}{\partial n}\phi(x)d\Gamma(x) \equiv \sum_{e=1}^{E}\sum_{j=1}^{J}\sum_{m=1}^{M_{ej}}\int_{-1}^{+1}\frac{\partial G(x,x_1)}{\partial n}N_j(\xi)e^{ik\psi_{jm}^e\cdot x}J^n(\xi)d\xi A_{jm}^e$$

$$(17)$$

We note that when Dirichlet and/or impedance boundary conditions are used the single layer potential term must also be included in the computation of the error

indicator. Having solved the system for the amplitudes A^e_{jm}, the potentials $\phi(x)$ and $\phi(x_1)$ are available by recombination from (10), and the entire right hand side of (16) may be readily evaluated to give the error indicator at an arbitrary boundary point x_1. R may be expected to be close to zero-valued when evaluated at $x_1 = x_0$, one of the original set of collocation points used in the solution of the problem. Typical behaviour is illustrated in Figure 1, in which the variation in R is plotted over one line element containing 13 uniformly distributed collocation points; R can be seen to be considerably lower at the original set of collocation points than at other locations on the element. The error indicator reaches a maximum approximately midway between each pair of collocation points x_0. It is further noticed consistently that the peaks in R increase towards the extremities of the element, a feature we attribute to the fact that the shape functions exhibit only C^0 continuity at the element boundaries. Therefore we consider the behaviour of R over an element e to be reasonably described by its value at just two points, x^e_L and x^e_R. These points are defined by their locations in parametric space, i.e.

$$\xi(x^e_L) = \frac{1}{2}(\xi(x_{0L}) + \xi(x_L)) \tag{18}$$

$$\xi(x^e_R) = \frac{1}{2}(\xi(x_{0R}) + \xi(x_R)) \tag{19}$$

where x_L and x_R are the two end node locations, and x_{0L}, x_{0R} are the non-nodal collocation points on the element that are closest to x_L and x_R respectively.
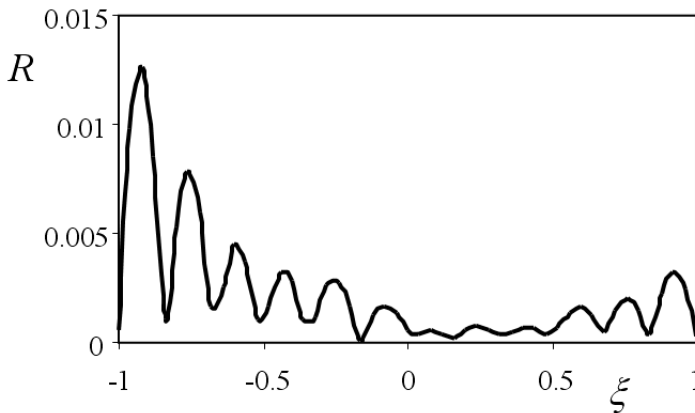

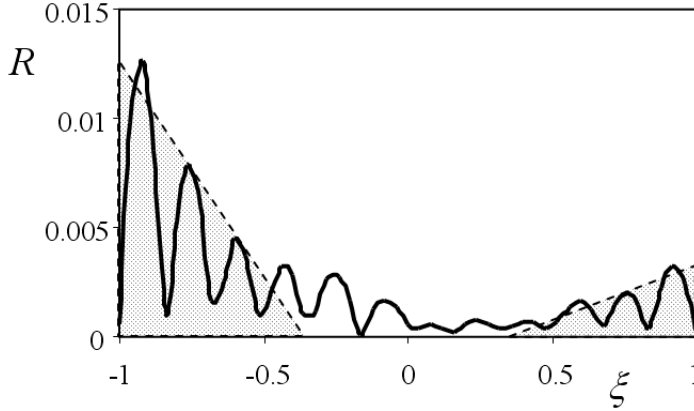Figure 1: Behaviour of error indicator over an element containing 13 collocation points

Figure 2: Showing the algorithm for approximating $||R||_1$

A suitable global error indicator might be based on a norm of R. Since $R(x_1) \geq 0, \forall x_1 \in \Gamma$, a 1-norm is sufficient, so that we define a global error norm

$$||R||_1 := \frac{1}{P} \oint R(x)d\Gamma(x) \tag{20}$$

where P is the perimeter of the boundary Γ. However, since it involves the evaluation of many highly oscillatory boundary integrals, this norm is costly to compute numerically. Fortunately, for the purpose of using it as a stopping criterion, the norm (20) is sufficiently well approximated by

$$||R||_1 \simeq \frac{1}{6P} \sum_{e=1}^{E} L^e[R(x_L^e) + R(x_R^e)] \tag{21}$$

where L^e is the length of element e. This corresponds to the combined area of the triangles of base equal to one third of the element length and height equal to $R(x_L^e)$ and $R(x_R^e)$, as illustrated in Figure 2. Numerical tests suggest that, using the definition (21), a stopping criterion $||R||_1 < 0.004$ is generally suitable to obtain engineering accuracy of 0.01 in ε, the $L^2(\Gamma)$ relative error norm of the approximation for ϕ for a perfectly reflecting cylinder, for which the exact solution, ϕ^{ex}, is available in Morse and Feshbach (1981). Reducing the threshold value for the stopping criterion provides for improved accuracy of the converged solution. For completeness we define ε as

$$\varepsilon = \frac{||\phi - \phi^{ex}||_{L^2(\Gamma)}}{||\phi^{ex}||_{L^2(\Gamma)}} \tag{22}$$

In evaluating $||R||_1$ using (21) it is important to store the local values of the error indicator $R(x_L^e), R(x_R^e), e = 1, ..., E$ found at any of these sampling points, since they will be used as the local error indicator.

Although it includes a non-local integral operator, the error indicator (16) may also be viewed as having local properties since it is effectively the use of the BIE to compute the potential $\phi(x_1)$, and evaluation of the discrepancy between this computation and the recovery of $\phi(x_1)$ from the PU-BEM solution through (10). We can illustrate the effectiveness of local variation in R as a local error indicator using the perfectly reflecting cylinder. For a case in which 24 elements are used to model the cylinder, we computed for each element the values

$$\varepsilon^e = \frac{||\phi - \phi^{ex}||_{L^2(\Gamma_e)}}{||\phi^{ex}||_{L^2(\Gamma_e)}} \tag{23}$$

$$||R||_1^e = \frac{L^e}{6P}[R(x_L^e) + R(x_R^e)] \tag{24}$$

These values, normalised by the maxima $max(\varepsilon^e, e = 1, ..., 24)$ and $max(||R||_1^e, e = 1, ..., 24)$ are plotted in Figure 3. There is a clear correlation, which we interpret as a justification to use R as a local error indicator.
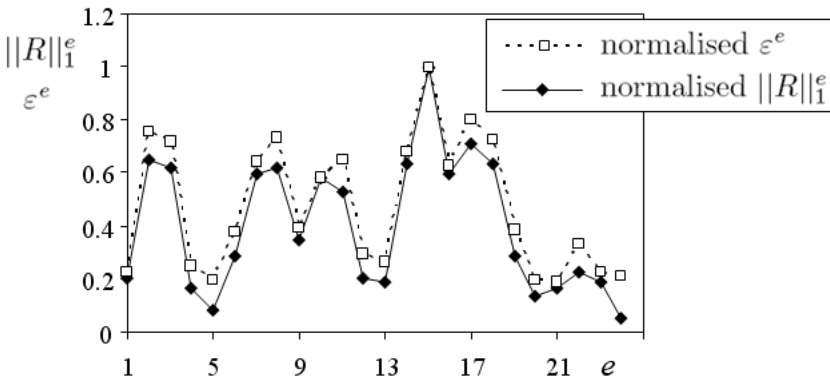

Figure 3: Variation of ε^e and $||R||_1^e$ over a 24 element model

In each adaptive iteration, new waves are added to the approximation space at nodes suggested by the local variation in the error indicator. New rows and columns are appended to the system matrix and a new solution is obtained. In the current work, since the evaluation of the boundary integrals incurs a large majority of the computational cost of the PU-BEM for typical problems, the complete set of equations is solved at each adaptive iteration. Further work is justified in incremental solution

schemes that might be iterative or involve an updated decomposition of the growing system matrix. Such schemes are likely to require preconditioning. The major benefit of the scheme is to end up with an approximation space that is optimised for the problem at hand such that confidence is gained in the solution accuracy while the number of oscillatory integral evaluations is effectively minimised.

4 Implementation

Different strategies have been tested for the *p*-adaptive enrichment in response to the local behaviour of R. It has been noted by Trevelyan, Bettess, and Perrey-Debain (2004) that the residual error indicator lacks the characteristic smoothness of Figure 1 when the plane wave basis is non-uniform. We suppose this to be an artefact of some interference between the waves in the basis at different nodes. The somewhat enhanced quality of the solution for a uniform basis is exploited in the final algorithm, in which the following steps are carried out in each adaptive iteration:

1. determine $R(x_L^e), R(x_R^e), e = 1, ..., E$ from (16) and, in the same process, assemble the global error norm $||R||_1$ from (21).

2. if $||R||_1 < 0.004$ the stopping criterion has been satisfied. Recover the potential solution from (10) and stop.

3. determine the total number of waves, n_u, that would be required to be added in order to reach a uniform basis at all nodes. If the model is already at a uniform basis, n_u takes the value of the total number of nodes, otherwise

$$n_u = \sum_{e=1}^{E} \sum_{j=1}^{J-1} M_{max} - M_{ej} \qquad (25)$$

    where $M_{max} = max(M_{ej}, e = 1, ..., E, j = 1, ..., J)$.

4. make a list of all nodes adjacent to sampling points $x_1 \in \{x_L^e, x_R^e, e = 1, ..., E\}$ at which $R(x_1) > R_{max}$. Here, R_{max} is a threshold to be determined by numerical tests. Let there be n_a such nodes in the list.

5. if $n_a > 0.75 n_u$ replace the list of nodes generated in step 4 by a list of length n_u, generated in step 3, that would bring about a uniform basis $M_{ej} = M_{max}, e = 1, ..., E, j = 1, ..., J$.

6. work down the list of nodes. At each, add a new wave in between two existing plane waves such that the basis becomes $\left\{ e^{ik\psi_{jm}^e \cdot x}, m = 1, ..., M_{ej} + 1 \right\}$, and increment by 1 the value of M_{ej}.

7. define new collocation points in the same number as the added degrees of freedom.

8. evaluate the boundary integrals required to populate the new rows and columns in K.

9. update required entries in the sparse matrix W to include the contributions of the newly added waves.

10. solve the enlarged PU-BEM system (13) for all plane wave amplitudes.

11. return to step 1.

The initial plane wave basis at all nodes j on all elements e comprises M_{ej}^1 wave directions uniformly spaced around the unit circle, i.e.

$$\psi_{jm}^e = (cos\theta_{jm}^e, sin\theta_{jm}^e), \quad \theta_{jm}^e = \frac{2\pi(m-1)}{M_{ej}^1} + \delta\theta, \quad m = 1,...,M_{ej}^1 \tag{26}$$

The value of M_{ej}^1 is determined to give an appropriate meshing efficiency $\tau \simeq 2.1$, where τ is the number of degrees of freedom used to model a portion of boundary Γ spanning one wavelength. We recall that $\tau = 10$ is the usual heuristic rule for FEM and BEM approximations to wave problems using a piecewise polynomial basis.

At the start of the analysis, we initialise counting parameters $p_{ej} = 1$, $q_{ej} = 1$ for all nodes. The following algorithm is used in step 6 of subsequent adaptive iterations to define the direction of a single plane wave direction in between existing directions at a node.

1. introduce a new plane wave in a direction

    $$\theta_{jm} = \frac{p_{ej}\pi}{q_{ej}M_{ej}^1} + \delta\theta \tag{27}$$

    where m is taken as $M_{ej} + 1$. The associated unit vector ψ_{jm}^e is defined as in (26), and M_{ej} is incremented by 1.

2. modify values of p_{ej} and q_{ej} according to:

    (a) if $p_{ej} + 2 < 2q_{ej}M_{ej}^1$, then let $p_{ej} = p_{ej} + 2$ and $q_{ej} = q_{ej}$

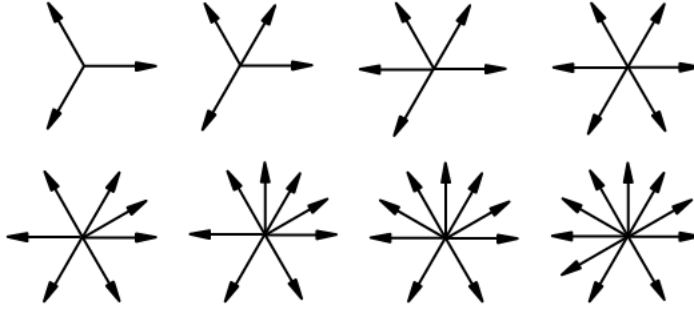   (b) if $p_{ej} + 2 \geq 2q_{ej}M_{ej}^1$, then let $p_{ej} = 1$ and $q_{ej} = 2q_{ej}$

Figure 4: Progressive addition of waves (case $M_{ej}^1 = 3$ shown)

This algorithm sequentially adds waves to bisect adjacent pairs of waves and will continue to find the next bisector at each new addition. This is illustrated in Figure 4 for the first eight iterations for the case $M_{ej}^1 = 3$. Numerical tests have shown that a moderate asymmetry of the plane wave basis is not detrimental to the solution obtained.

At each iteration, in step 7 a set of additional collocation points is defined so that the total number of collocation points is equal to the number of unknowns. We locate the new points on the elements on which new plane waves are added, but confine the new points to the interval $\xi \in (\xi(x_{0L}), \xi(x_{0R}))$ in the present study in order to maintain a consistent definition of the global error norm (21).

4.1 Mesh considerations

It is clear from the presentation of the PU-BEM in Section 2, that the degrees of freedom in the analysis are represented by the amplitudes of a set of plane wave directions forming a basis for the approximation space at each node. Simple consideration of the perimeter, P, and of the required number of degrees of freedom per wavelength, τ, will suggest that a total number of degrees of freedom, N_d, where

$$N_d = \frac{P\tau}{\lambda}, \tag{28}$$

should be provided. Let us assume, for simplicity, that every node is provided with a uniform basis comprising M wave directions, and that there is a total of N nodes. N_d is then given by MN. Thus we have flexibility to accumulate the required number of degrees of freedom by various combinations of M and N. Early developments in the PU-BEM for Helmholtz problems (Perrey-Debain, Trevelyan, and Bettess (2003a)) showed that the accuracy of the method is influenced by this

choice, and concluded that convergence is optimised if N is minimised and M maximised. Best results were shown for $N = 1$, i.e. using a single element to model the entire closed boundary.

With the introduction of adaptivity, we have a conflicting demand, since the algorithm progresses by improving the model in a *localised* way. For this reason, we proceed into Section 5 to present examples having a larger N and smaller M than would be suggested by the 2003 study.

5   Results

The adaptive PU-BEM algorithm is illustrated in this section using two example problems: scattering of a plane wave by a circular cylinder and by a system of three cylinders of different diameters. The cylinders are perfectly reflecting as is assumed for simplicity in the theoretical development earlier in this paper; for more general cases the algorithm would simply be extended by including the single layer potential in the residual error indicator (16).

5.1   *Scattering by a circular cylinder*

Consider a cylindrical scatterer of radius $a = 10$ impinged by an incident wave of unit amplitude and wavelength $\lambda = 0.5$ (consistent units are assumed) propagating in direction (1,0). This example provides $ka = 125$. The cylinder is modelled by 24, 3-noded boundary elements, and the initial model is provided with $M_{ej}^1 = 6$ for all nodes, giving 288 degrees of freedom ($\tau = 2.29$ degrees of freedom per wavelength). This initial analysis has error norm $||R||_1 = 0.00548$. The adaptive algorithm converges in a single further iteration to finish at $||R||_1 = 0.00125$, which corresponds to a 0.33% error in the $L^2(\Gamma)$ relative error norm on the potential solution in comparison with the analytical solution in Morse and Feshbach (1981). In the converged solution the model has 313 degrees of freedom at $\tau = 2.49$. The total run time is comparable to the non-adaptive solution using a uniform basis $M = 7$; in fact it shows a small reduction of 4% in run time.

The geometry-normalised wavenumber $ka = 125$ in this example is sufficiently high that the initial model, exhibiting $\tau = 2.29$, is itself able to produce a reasonably accurate solution. The adaptive procedure has fine-tuned the solution with a more efficient use of resources than simply running again with a larger M applied uniformly. If we retain the 24-element mesh but double the wavelength to give a reduced $ka = 62.8$, the initial model exhibits $M_{ej}^1 = 3$ for all nodes, giving 144 degrees of freedom ($\tau = 2.29$ degrees of freedom per wavelength). Three adaptive iterations are required in order to achieve convergence. In these three iterations the global error norm is found to be 0.0124, 0.00401 (just missing the stopping

criterion) and 0.00210. Again, the run-time shows a small saving of 12.3% over the most efficient non-adaptive solution that achieves the same accuracy using a uniform basis. It is to be expected that the run times for adaptive and non-adaptive solutions are comparable, since the gains that are made by reducing the number of oscillatory integral evaluations are offset by the requirement to solve the system of equations multiple times.

Figure 5 shows plots of R over the boundary Γ for the solutions of the three adaptive iterations. In these graphs the horizontal axis is defined by angle θ taken clockwise around the scatterer, having $\theta = 0$ at the first point of contact with the incident wave. The asymmetry of the error indicator about $\theta = \pi$ may be attributed to the random definition of the Chief points inside the scatterer.
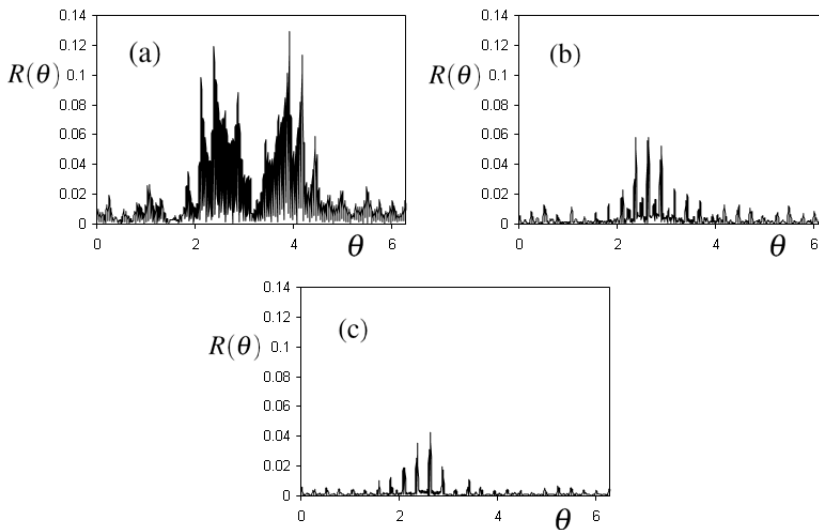

Figure 5: Evolution of error indicator for cylinder problem taking $ka = 62.8$. (a) first iteration, (b) second iteration, (c) third and final iteration

It should be noted that the calculation of R over the boundary, enabling the plotting of Figure 5, is made for illustrative purposes only, and the reader is reminded that in this scheme the error indicator is required only at two points per element, as shown in equation (21).

For scattering by a single cylinder the behaviour of the PU-BEM is well understood so that, using a non-adaptive solution using a uniform basis of M plane waves at each node, it is possible to select a suitable value of M a priori that experience suggests will give any desired accuracy. The principal advantage of the adaptive

scheme is found in more general problems, where the choice of an appropriate *M* is not so clear and cannot be deduced from experience as for a single cylinder problem. We proceed now to present such a case.

5.2 Scattering by three cylinders

Consider a set of cylindrical scatterers in an infinite acoustic medium, being impinged by an incident plane wave of unit amplitude and wavelength $\lambda = 0.25$, propagating in direction (1,0). The geometry and meshing for the scatterers are defined in Table 1. All elements have three nodes, and the entire boundary to the problem, Γ, is defined as $\Gamma = \Gamma_1 \cup \Gamma_2 \cup \Gamma_3$.

Table 1: Geometric definition of the three cylinders

Scatterer	Centre	Radius	No. of elements	Boundary
1	(0, 0)	1	8	Γ_1
2	(2, 3)	2	16	Γ_2
3	(4, -2)	3	24	Γ_3

The convergence of the global error norm $||R||_1$, from $||R||_1 = 0.1485$ for the initial analysis ($M = 4, \tau = 2.54$) to achieve convergence in the 4th iteration at $||R||_1 = 0.00264$, is shown in Figure 6. Convergence is achieved using $N_d = 631$ at $\tau = 4.18$. Contours of the converged solution $Re(\phi)$ are shown in Figure 7, and show reflection from the illuminated surfaces, a clear shadow region to the right, diffraction around the sides of the scatterers and a complicated region of multiple reflections between the three cylinders. This complication is emphasised by plotting $|\phi|$ on Γ_2, as shown in Figure 8. In Figure 9, we plot over Γ_2 a measure, ε_2, of the difference between the converged adaptive solution (plotted in Figure 8) and the solution $\bar{\phi}$ obtained using a direct collocation BEM approximation using 1520 degrees of freedom at $\tau = 10.1$. This measure is defined by

$$\varepsilon_2 = \frac{||\phi| - |\bar{\phi}||}{|\bar{\phi}|_{max}} \tag{29}$$

We can measure the improvement in accuracy as the adaptive scheme progresses using a relative error, ε_3, defined as

$$\varepsilon_3 = \frac{||\phi - \bar{\phi}||_{L^2(\Gamma)}}{||\bar{\phi}||_{L^2(\Gamma)}} \tag{30}$$

The evolution in ε_3 with iteration number is shown in Figure 10. The most efficient non-adaptive solution to achieve this accuracy uses $M = 7$ and exhibits $\tau = 4.46$. In
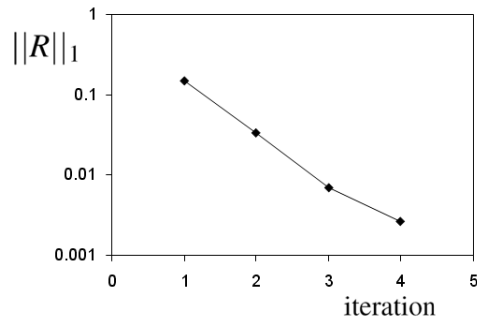
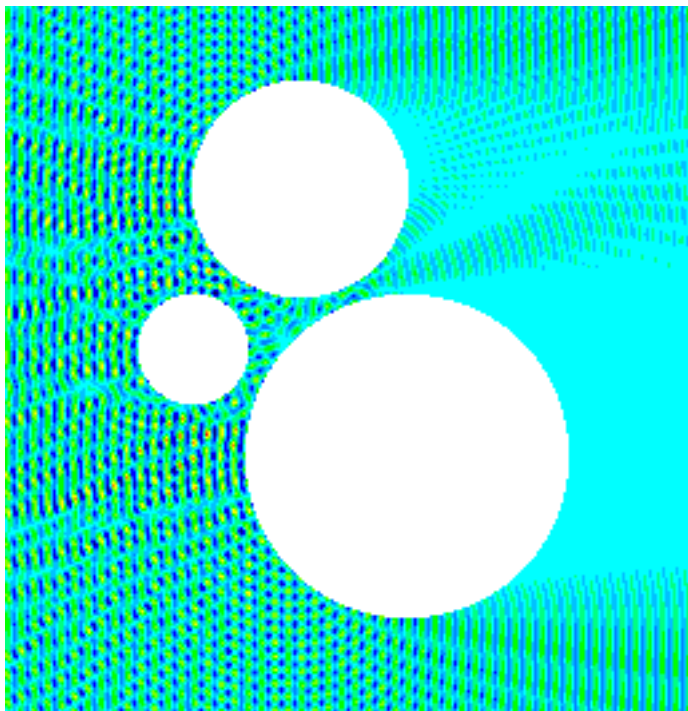Figure 6: Evolution of global error norm for three cylinder problem

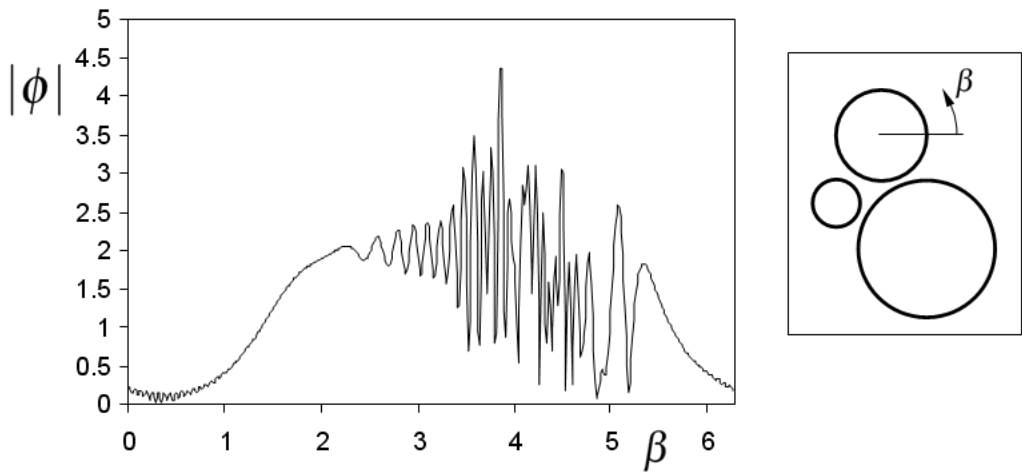

Figure 7: Real part of the potential (converged solution)

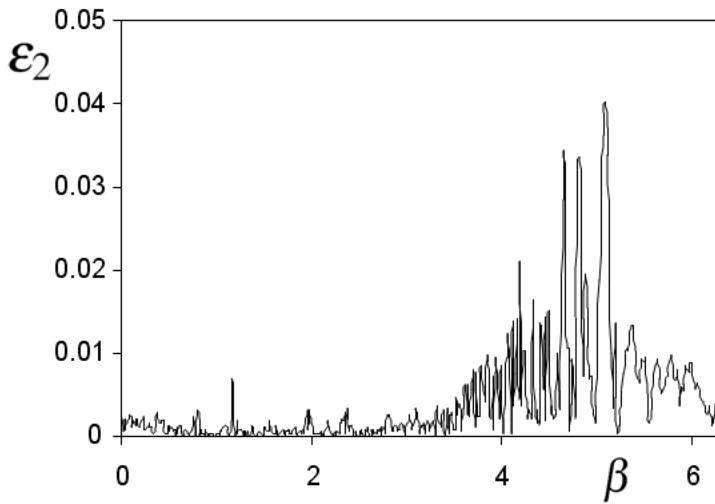Figure 8: Magnitude of potential on boundary of scatterer 2

Figure 9: Difference measure ε_2 on boundary of scatterer 2

this case the run-time for the adaptive solution is somewhat greater (by 19%) than this non-adaptive solution, but it must be remembered that the required value of *M* for non-adaptive solutions is not known in advance and that multiple runs may be required to confirm convergence.
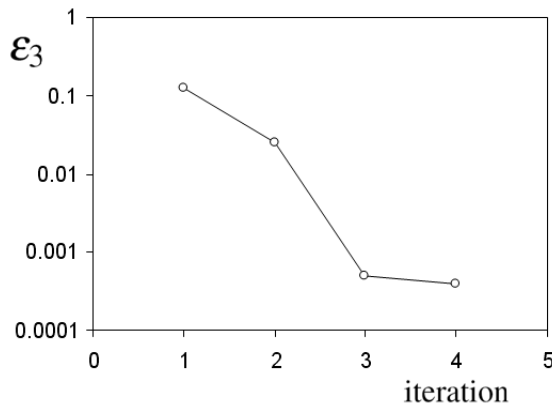

Figure 10: Evolution of ε_3 for three cylinder problem

6   Conclusions

An adaptive form of the Partition of Unity Boundary Element Method (PU-BEM) has been presented for the solution of wave scattering problems. The approach involves a residual based error indicator that has both global and local properties, allowing it to be used as a stopping criterion and also as an indicator of areas of a model in which further enrichment is required. The residual is normalised by the amplitude of the incident wave in scattering problems, allowing a single threshold to be used for general scattering problems. An efficient approximation to the global error norm is presented, requiring evaluation at only two points on each element.

The adaptive scheme is of the p-adaptive character; the mesh remains unaltered but the approximation space is enriched in each iteration, in regions suggested by the local variation in the error indicator, by the addition of an extra plane wave to the basis. An algorithm is presented for the iterative addition of new waves in between existing wave directions.

Illustrative examples demonstrate the convergence of the algorithm to solutions that exhibit at least engineering accuracy. More accuracy may be obtained simply by modifying the threshold value for the global error norm that is used as a stopping criterion. Run times for the adaptive solution are comparable to those of the

most efficient non-adaptive solution that achieves the same accuracy using a uniform basis. The adaptive scheme is beneficial in that it removes the requirement to estimate in advance the required number of plane waves with which to enrich the approximation space; such an estimate is not always straightforward.

Further work is required to extend the algorithm to scattering problems in 3D, where greater benefits are expected.

References

Abboud, T.; Nédélec, J.; Zhou, B. (1995): Improvement of the integral equation method for high frequency problems. In *3rd Intl. Conf. on Mathematical Aspects of Wave Propagation Phenomena*, pp. 178–187. SIAM, Philadelphia.

Anand, A.; Boubendir, Y.; Ecevit, F.; Reitich, F. (2006):   Analysis of multiple scattering iterations for high-frequency scattering problems. ii: The three-dimensional scalar case. *Preprint 147/2006, Max Planck Institute*.

Bebendorf, M. (2000):   Approximation of boundary element matrices. *Numer. Math.*, vol. 86, pp. 565–589.

Bériot, H.; Perrey-Debain, E.; Ben Tahar, M.; Vayssade, C. (2010):   Plane wave basis in Galerkin BEM for bidimensional wave scattering. *Engineering Analysis with Boundary Elements*, vol. 34, pp. 130–143.

Brancati, A.; Aliabadi, M.; Benedetti, I. (2009):   Hierarchical Adaptive Cross Approximation GMRES technique for solution of acoustic problems using the boundary element method. *CMES: Computer Modeling in Engineering and Sciences*, vol. 43, pp. 149–172.

Brebbia, C.; Ciskowski, R. (1991):   *Boundary Element Methods in Acoustics*. CMP and Elsevier Applied Science, Southampton.

Bruno, O.; Geuzaine, C.; Munro, J.; Reitich, F. (2004):   Prescribed error tolerances within fixed computational times for scattering problems of arbitrarily high frequency: the convex case. *Phil. Trans. Royal Soc. London A*, vol. 362, no. 1816, pp. 629–645.

Burton, A.; Miller, G. (1971):   The application of integral equation methods to the numerical solution of some exterior boundary-value problems. *Phil. Trans. Royal Soc. London A*, vol. 323, pp. 201–210.

Cessenat, O.; Després, B. (1998): Application of the ultra-weak variational formulation of elliptic PDE's to the two-dimensional Helmholtz problem. *SIAM J. Numer. Anal.*, vol. 35, pp. 255–299.

Chandrasekhar, B.; Rao, S. (2008): A faster method of moments solution to double layer formulation of acoustic scattering. *CMES: Computer Modeling in Engineering and Sciences*, vol. 33, pp. 199–214.

Chew, W.; Jin, J.; Michielssen, E.; Song, J. (1997): Fast solution methods in electromagnetics. *IEEE Trans Antennas Propag*, vol. 45, pp. 533–543.

Darve, E. (2000): The fast multipole method: numerical implementation. *Journal of Computational Physics*, vol. 1608, pp. 195–240.

de la Bourdonnaye, A. (1994): A microlocal discretization method and its utilization for a scattering problem. *Comptes Rendus de l'Académie des Sciences., Paris, Série I*, vol. 38, pp. 385–388.

Dominguez, V.; Graham, I.; Smyshlyaev, V. (2007): A hybrid numerical-asymptotic boundary integral method for high-frequency acoustic scattering. *Numer. Math.*, vol. 106, pp. 471–510.

Farhat, C.; Harari, I.; Franca, L. (2001): The discontinuous enrichment method. *Computer Methods in Applied Mechanics and Engineering*, vol. 190, pp. 6455–6479.

Honnor, M.; Trevelyan, J.; Huybrechs, D. (2009): Numerical evaluation of 2D partition of unity boundary integrals for Helmholtz problems. *Journal of Computational and Applied Mathematics*, vol. to appear.

Huybrechs, D.; Vandewalle, S. (2006): On the evaluation of highly oscillatory integrals by analytic continuation. *SIAM J. Numer. Anal.*, vol. 44, pp. 1026–1048.

Kim, T.; Dominguez, V.; Graham, I.; Smyshlyaev, V. (2009): Recent progress on hybrid numerical-asymptotic moethods for high-frequency scattering problems. In *Proc. 7th UK Conf. on boundary integral methods*, pp. 15–23. Univ. of Nottingham.

Ladevèze, P.; Sourcis, B.; Riou, H.; Faverjon, B. (2008): An adaptive computational "wave" approach. In *Proc. WCCM8/ECCOMAS, Venice, Italy*.

Laghrouche, O.; Bettess, P.; Astley, R. (2002): Modelling of short wave diffraction problems using approximating systems of plane waves. *International Journal for Numerical Methods in Engineering*, vol. 54, pp. 1501–1533.

Laghrouche, O.; Bettess, P.; Perrey-Debain, E.; Trevelyan, J. (2003): Plane wave basis finite elements for wave scattering in three dimensions. *Communications in Numerical Methods in Engineering*, vol. 19, no. 9, pp. 715–723.

Langdon, S.; Chandler-Wilde, S. (2006): A wavenumber independent boundary element method for as acoustic scattering problem. *SIAM J. Numerical Analysis*, vol. 43, pp. 2450–2477.

Massimi, P.; Tezaur, R.; Farhat, C. (2008): A discontinuous enrichment method for three-dimensional multiscale harmonic wave propagation problems in multi-fluid and fluid-solid media. *International Journal for Numerical Methods in Engineering*, vol. 76, pp. 400–425.

Melenk, J.; Babuška, I. (1996): The partition of unity finite element method. basic theory and applications. *Computer Methods in Applied Mechanics and Engineering*, vol. 139, pp. 289–314.

Mohsen, A.; Hesham, M. (2006): An efficient method for solving the nonuniqueness problem in acoustic scattering. *Communications in Numerical Methods in Engineering*, vol. 22, pp. 1067–1076.

Morse, P.; Feshbach, H. (1981): *Methods of Theoretical Physics*. Feshbach Publishing.

Ortiz, P.; Sanchez, E. (2000): An improved partition of unity finite element model for diffraction problems. *International Journal for Numerical Methods in Engineering*, vol. 50, pp. 2727–2740.

Perrey-Debain, E.; Laghrouche, O.; Bettess, P.; Trevelyan, J. (2004): Plane wave basis finite elements and boundary elements for three dimensional wave scattering. *Phil. Trans. Royal Society London A*, vol. 362, no. 1816, pp. 561–577.

Perrey-Debain, E.; Trevelyan, J.; Bettess, P. (2002): New special wave boundary elements for short wave problems. *Communications in Numerical Methods in Engineering*, vol. 18, no. 4, pp. 259–268.

Perrey-Debain, E.; Trevelyan, J.; Bettess, P. (2003): Plane wave approximation in the direct collocation boundary element method for radiation and wave scattering: numerical aspects and applications. *Journal of Sound and Vibration*, vol. 261, no. 5, pp. 839–858.

Perrey-Debain, E.; Trevelyan, J.; Bettess, P. (2003): Wave boundary elements for acoustic computations. *Journal of Computational Acoustics*, vol. 11, no. 2, pp. 305–321.

Riou, H.; Ladevèze, P.; Sourcis, B. (2008): The multiscale VTCR approach applied to acoustics problems. *Journal of Computational Acoustics*, vol. 16(4), pp. 487–505.

Schenck, H. (1968): Improved integral formulation for acoustic radiation problems. *Journal of the Acoustical Society of America*, vol. 44, pp. 41–58.

Soares, D. (2009): Numerical modelling of electromagnetic wave propagation by Meshless Local Petrov-Galerkin formulations. *CMES: Computer Modeling in Engineering and Sciences*, vol. 50, pp. 97–114.

Strouboulis, T.; Babuška, I.; Hidajat, R. (2006): The generalized finite element method for Helmholtz equation: Theory, computation and open problems. *Computer Methods in Applied Mechanics and Engineering*, vol. 195, pp. 4711–4731.

Trevelyan, J. (2007): Numerical steepest descent evaluation of 2D partition of unity boundary integrals for Helmholtz problems. *Oberwolfach Report*, vol. 5/2007, pp. 74–76.

Trevelyan, J.; Bettess, P.; Perrey-Debain, E. (2004): Experiments in adaptive selection of plane wave basis directions for wave boundary elements. In *Developments in Mechanics of Structures and Materials*.

Trevelyan, J.; Honnor, M. (2009): A numerical coordinate transformation for efficient evaluation of oscillatory integrals over wave boundary elements. *J. Integral Equations and Appl.*, vol. 21, pp. 447–468.